

Subcell *a posteriori* limitation for DG scheme through flux reconstruction

François Vilar

Alexander Grothendieck Montpellier Institute
Montpellier University

July 2-9, 2018



IMAG
INSTITUT MONTPELLIERAIN
ALEXANDER GROTHENDIECK



- 1 Introduction
- 2 DG as a subcell finite volume
- 3 *A posteriori* subcell limitation
- 4 Numerical results

History

- Introduced by Reed and Hill in 1973 in the frame of the neutron transport
- Major development and improvements by B. Cockburn and C.-W. Shu in a series of seminal papers

Procedure

- Local variational formulation
- Piecewise polynomial approximation of the solution in the cells
- Choice of the numerical fluxes
- Time integration

Advantages

- Natural extension of Finite Volume method
- Excellent analytical properties (L_2 stability, hp -adaptivity, ...)
- Extremely high accuracy (superconvergent for scalar conservation laws)
- Compact stencil (involve only face neighboring cells)

1D scalar conservation law

- $\frac{\partial u}{\partial t} + \frac{\partial F(u)}{\partial x} = 0, \quad (x, t) \in \omega \times [0, T]$
- $u(x, 0) = u_0(x), \quad x \in \omega$

$(k + 1)^{\text{th}}$ order discretization

- $\{\omega_i\}_i$ a partition of ω , such that $\omega_i = [x_{i-\frac{1}{2}}, x_{i+\frac{1}{2}}]$
- $0 = t^0 < t^1 < \dots < t^N = T$ a partition of the temporal domain $[0, T]$
- $u_h(x, t)$ the numerical solution, such that $u_h|_{\omega_i} = u_h^i \in \mathbb{P}^k(\omega_i)$

$$u_h^i(x, t) = \sum_{m=1}^{k+1} u_m^i(t) \sigma_m(x)$$

- $\{\sigma_m\}_m$ a basis of $\mathbb{P}^k(\omega_i)$

Variational formulation on ω_j

- $\int_{\omega_j} \left(\frac{\partial u}{\partial t} + \frac{\partial F(u)}{\partial x} \right) \psi \, dx$ with $\psi(x)$ a test function

Integration by parts

$$\bullet \int_{\omega_i} \frac{\partial u}{\partial t} \psi \, dx - \int_{\omega_i} F(u) \frac{\partial \psi}{\partial x} \, dx + \left[F(u) \psi \right]_{x_{i-\frac{1}{2}}}^{x_{i+\frac{1}{2}}} = 0$$

Approximated solution

- Substitute u by u_h^i
- Take ψ among the basis function σ_p

$$\bullet \sum_{m=1}^{k+1} \frac{\partial u_m^i}{\partial t} \int_{\omega_i} \sigma_m \sigma_p \, dx = \int_{\omega_i} F(u_h^i) \frac{\partial \sigma_p}{\partial x} \, dx - \left[\mathcal{F} \sigma_p \right]_{x_{i-\frac{1}{2}}}^{x_{i+\frac{1}{2}}}$$

Numerical flux

- $\mathcal{F}_{i+\frac{1}{2}} = \mathcal{F} \left(u_h^i(x_{i+\frac{1}{2}}, t), u_h^{i+1}(x_{i+\frac{1}{2}}, t) \right)$
- $\mathcal{F}(u, v) = \frac{F(u) + F(v)}{2} - \frac{\gamma(u, v)}{2} (v - u)$
- $\gamma(u, v) = \max(|F'(u)|, |F'(v)|)$

Local Lax-Friedrichs

Subcell resolution of DG scheme

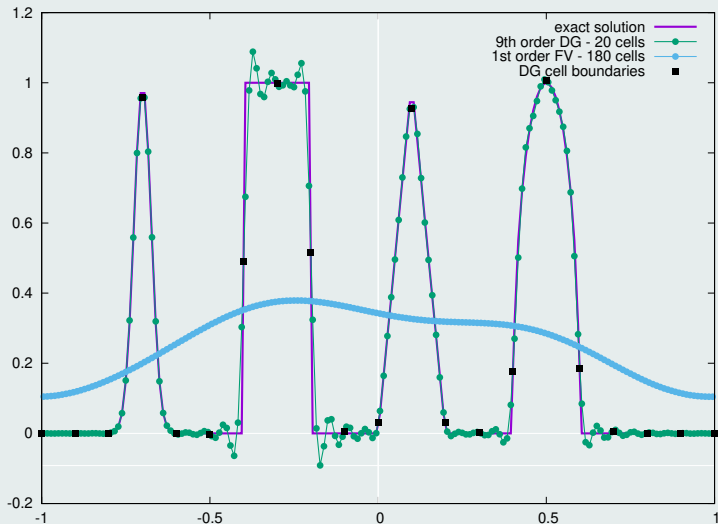


Figure : Linear advection of composite signal after 4 periods

Subcell resolution of DG scheme

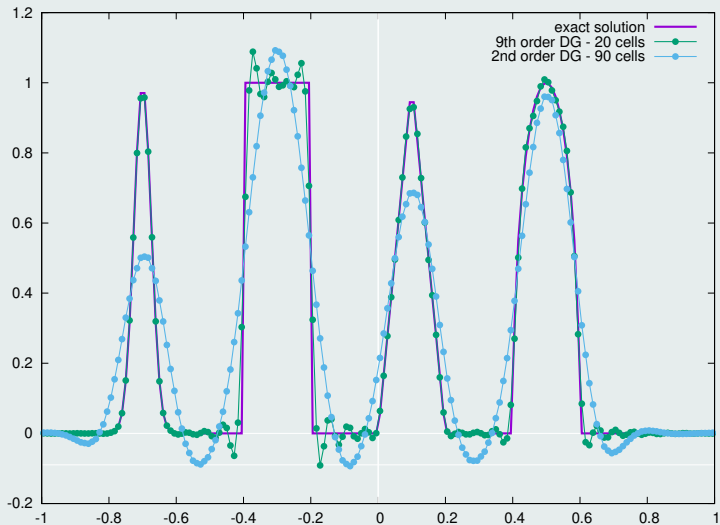


Figure : Linear advection of composite signal after 4 periods

Gibbs phenomenon

- High-order schemes leads to spurious oscillations near discontinuities
- Leads potentially to nonlinear instability, non-admissible solution, crash
- Vast literature of how prevent this phenomenon to happen:

⇒ *a priori* and ***a posteriori*** limitations

A priori limitation

- Artificial viscosity
- Flux limitation
- Slope/moment limiter
- Hierarchical limiter
- ENO/WENO limiter

A posteriori limitation

- MOOD (“Multi-dimensional Optimal Order Detection”)
- Subcell finite volume limitation
- **Subcell limitation through flux reconstruction**

Admissible numerical solution

- Maximum principle / positivity preserving
- Prevent the code from crashing (for instance avoiding NaN)
- **Ensure the conservation of the scheme**

Spurious oscillations

- Discrete maximum principle
- Relaxing condition for smooth extrema

Accuracy

- Retain as much as possible the subcell resolution of the DG scheme
- Minimize the number of subcell solutions to recompute

- 1 Introduction
- 2 **DG as a subcell finite volume**
- 3 *A posteriori* subcell limitation
- 4 Numerical results

DG as a subcell finite volume

- Rewrite DG scheme as a specific finite volume scheme on subcells
- Exhibit the corresponding subcell numerical fluxes: **reconstructed flux**

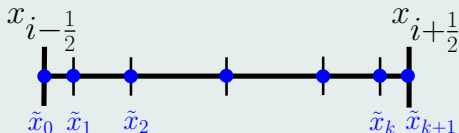
Variational formulation

$$\bullet \int_{\omega_i} \frac{\partial u_h^i}{\partial t} \psi \, dx = \int_{\omega_i} F(u_h^i) \frac{\partial \psi}{\partial x} \, dx - [\mathcal{F} \psi]_{x_{i-\frac{1}{2}}^{x_{i+\frac{1}{2}}}}, \quad \forall \psi \in \mathbb{P}^k(\omega_i)$$

- Substitute $F(u_h^i)$ with $F_h^i \in \mathbb{P}^{k+1}(\omega_i)$ (collocated or L_2 projection)

$$\bullet \int_{\omega_i} \frac{\partial u_h^i}{\partial t} \psi \, dx = - \int_{\omega_i} \frac{\partial F_h^i}{\partial x} \psi \, dx + [(F_h^i - \mathcal{F}) \psi]_{x_{i-\frac{1}{2}}^{x_{i+\frac{1}{2}}}}, \quad \forall \psi \in \mathbb{P}^k(\omega_i)$$

Subcell decomposition through $k + 2$ flux points



Subresolution basis functions

- ω_i is subdivided in $k + 1$ subcells $S_m^i = [\tilde{x}_{m-1}, \tilde{x}_m]$
- Let us introduce the $k + 1$ basis functions $\{\phi_m\}_m$ such that $\forall \psi \in \mathbb{P}^k(\omega_i)$

$$\int_{\omega_i} \phi_m \psi \, dx = \int_{S_m^i} \psi \, dx, \quad \forall m = 1, \dots, k + 1$$

- Let us define $\bar{\psi}_m = \frac{1}{|S_m^i|} \int_{S_m^i} \psi \, dx$ the subcell mean value

Local variational formulation

- $\int_{\omega_i} \frac{\partial u_h^i}{\partial t} \phi_m \, dx = - \int_{\omega_i} \frac{\partial F_h^i}{\partial x} \phi_m \, dx + \left[(F_h^i - \mathcal{F}) \phi_m \right]_{x_{i-\frac{1}{2}}}^{x_{i+\frac{1}{2}}}$
- $\frac{\partial \bar{u}_m^i}{\partial t} = - \frac{1}{|S_m^i|} \left(\left[F_h^i \right]_{\tilde{x}_{m-1}}^{\tilde{x}_m} - \left[\phi_m (F_h^i - \mathcal{F}) \right]_{x_{i-\frac{1}{2}}}^{x_{i+\frac{1}{2}}} \right)$
- $\frac{\partial \bar{u}_m^i}{\partial t} = - \frac{1}{|S_m^i|} \left(\hat{F}_m^i - \hat{F}_{m-1}^i \right)$

Subcell finite volume

Linear system

- $\widehat{F}_m^i - \widehat{F}_{m-1}^i = \left[F_h^i \right]_{\widetilde{x}_{m-1}}^{\widetilde{x}_m} - \left[\phi_m (F_h^i - \mathcal{F}) \right]_{x_{i-\frac{1}{2}}}^{x_{i+\frac{1}{2}}}, \quad \forall m = 1, \dots, k$
- $\widehat{F}_0^i = \mathcal{F}_{i-\frac{1}{2}}$ and $\widehat{F}_{k+1}^i = \mathcal{F}_{i+\frac{1}{2}}$

Reconstructed flux

- $\widehat{F}_m^i = F_h^i(\widetilde{x}_m) - C_{i-\frac{1}{2}}^{(m)} \left(F_h^i(x_{i-\frac{1}{2}}) - \mathcal{F}_{i-\frac{1}{2}} \right) - C_{i+\frac{1}{2}}^{(m)} \left(F_h^i(x_{i+\frac{1}{2}}) - \mathcal{F}_{i+\frac{1}{2}} \right)$
- $C_{i-\frac{1}{2}}^{(m)} = \sum_{p=m+1}^{k+1} \phi_p(x_{i-\frac{1}{2}})$ and $C_{i+\frac{1}{2}}^{(m)} = \sum_{p=1}^m \phi_p(x_{i+\frac{1}{2}})$

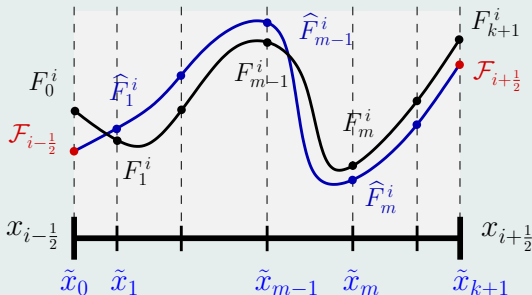
Correction terms for symmetric distribution of $\{\widetilde{x}_m\}_m$

- Let $\mathbf{B} \in \mathbb{R}^{k+1}$ be defined as $B_j = (-1)^{j+1} \frac{(k+1)(k+j)!}{(j!)^2(k+1-j)!}$
- $\widetilde{\xi}_m = \frac{\widetilde{x}_m - x_{i-\frac{1}{2}}}{x_{i+\frac{1}{2}} - x_{i-\frac{1}{2}}}, \quad \forall m = 0, \dots, k+1$
- $C_{i-\frac{1}{2}}^{(m)} = 1 - \left(\widetilde{\xi}_m, \dots, (\widetilde{\xi}_m)^{k+1} \right)^t \cdot \mathbf{B}$ and $C_{i+\frac{1}{2}}^{(m)} = C_{i-\frac{1}{2}}^{(k+1-m)}$

Subcell finite volume equivalent to DG

- $$\int_{\omega_i} \frac{\partial u_h^i}{\partial t} \psi \, dx = \int_{\omega_i} F(u_h^i) \frac{\partial \psi}{\partial X} \, dx - [\mathcal{F} \psi]_{x_{i-\frac{1}{2}}}^{x_{i+\frac{1}{2}}}, \quad \forall \psi \in \mathbb{P}^k(\omega_i)$$
- $$\frac{\partial \bar{u}_m^i}{\partial t} = -\frac{1}{|S_m^i|} (\widehat{F}_m^i - \widehat{F}_{m-1}^i), \quad \forall m = 1, \dots, k+1$$
- $$\widehat{F}_m^i = F_h^i(\tilde{x}_m) - C_{i-\frac{1}{2}}^{(m)} \left(F_h^i(x_{i-\frac{1}{2}}) - \mathcal{F}_{i-\frac{1}{2}} \right) - C_{i+\frac{1}{2}}^{(m)} \left(F_h^i(x_{i+\frac{1}{2}}) - \mathcal{F}_{i+\frac{1}{2}} \right)$$

Reconstructed flux taking into account flux jumps



Pointwise evolution scheme

- $\int_{\omega_i} \phi_m \left(\frac{\partial u_h^i}{\partial t} + \frac{\partial \widehat{F}_h^i}{\partial x} \right) dx = 0, \quad \forall m = 1, \dots, k+1$
 - $\int_{\omega_i} \psi \left(\frac{\partial u_h^i}{\partial t} + \frac{\partial \widehat{F}_h^i}{\partial x} \right) dx = 0, \quad \forall \psi \in \mathbb{P}^k(\omega_i) \implies \frac{\partial u_h^i}{\partial t} + \frac{\partial \widehat{F}_h^i}{\partial x} = \mathcal{O}_{\mathbb{P}^k}$
- $$\forall m = 1, \dots, k+1, \quad \frac{\partial u_h^i(x_m, t)}{\partial t} + \frac{\partial \widehat{F}_h^i(x_m, t)}{\partial x} = 0$$

Reconstructed flux

- $\widehat{F}_h^i = F_h^i + \left(F_h^i(x_{i-\frac{1}{2}}) - \mathcal{F}_{i-\frac{1}{2}} \right) g_{LB}(x) + \left(F_h^i(x_{i+\frac{1}{2}}) - \mathcal{F}_{i+\frac{1}{2}} \right) g_{RB}(x)$
- The $g_{LB}(x)$ and $g_{RB}(x)$ are the correction functions taking into account the flux discontinuities
- To recover DG scheme, the correction functions writes

$$g_{LB}(x) = \sum_{m=0}^{k+1} C_{i-\frac{1}{2}}^{(m)} L_m(x) \quad \text{and} \quad g_{RB}(x) = \sum_{m=0}^{k+1} C_{i+\frac{1}{2}}^{(m)} L_m(x)$$

Reconstructed flux

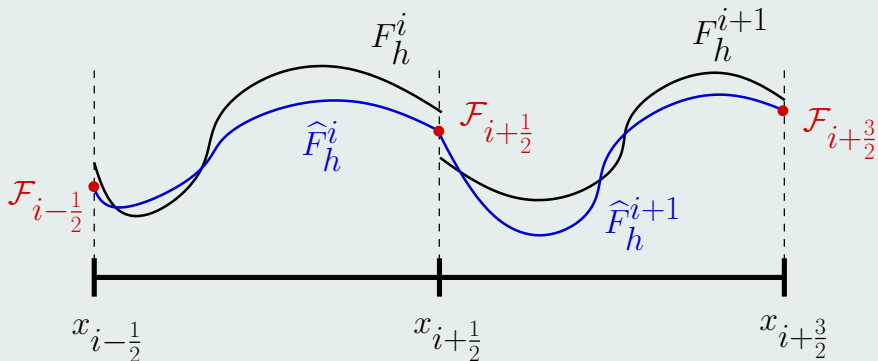


Figure : Reconstructed flux taking into account flux jumps

Flux reconstruction / CPR

- In the case of DG scheme, the correction functions $g_{LB}(x)$ and $g_{RB}(x)$ are nothing but the right and left Radau \mathbb{P}^k polynomials



H. T. HUYNH, *A Flux Reconstruction Approach to High-Order Schemes Including Discontinuous Galerkin Methods*. 18th AIAA Computational Fluid Dynamics Conference Miami, 2007.



Z.J. WANG and H. GAO, *A unifying lifting collocation penalty formulation including the discontinuous Galerkin, spectral volume/difference methods for conservation laws on mixed grids*. JCP, 2009.

- In the FR/CPR approach, the reconstructed flux is used pointwisely at some solution points to resolve the PDE

Subcell finite volume

- The reconstructed flux is used as a numerical flux for the subcell finite volume scheme
- This demonstration is not restricted to the flux collocation case
- The correction terms are very simple and explicitly defined
- There is no need to make use of Radau polynomial

- 1 Introduction
- 2 DG as a subcell finite volume
- 3 A *posteriori* subcell limitation**
- 4 Numerical results

RKDG scheme

- SSP Runge-Kutta: convex combinations of first-order forward Euler
- For sake of clarity, we focus on forward Euler time stepping

- $$u_h^{i,n}(x) = \sum_{m=1}^{k+1} u_m^{i,n} \sigma_m(x)$$

- $$\int_{\omega_i} u_h^{i,n+1} \sigma_p dx = \int_{\omega_i} u_h^{i,n} \sigma_p dx + \Delta t \left(\int_{\omega_i} F_h^{i,n} \frac{\partial \sigma_p}{\partial x} dx - [\mathcal{F}^n \sigma_p]_{x_{i-\frac{1}{2}}}^{x_{i+\frac{1}{2}}} \right)$$

Projection on subcells of RKDG solution

- A k^{th} degree polynomial is uniquely defined by its $k + 1$ submean values
- Introducing the matrix $\mathbf{\Pi}$ defined as $\pi_{mp} = \frac{1}{|S_m^i|} \int_{S_m^i} \sigma_p dx$, then

$$\mathbf{\Pi} \begin{pmatrix} u_1^{i,n} \\ \vdots \\ u_{k+1}^{i,n} \end{pmatrix} = \begin{pmatrix} \bar{u}_1^{i,n} \\ \vdots \\ \bar{u}_{k+1}^{i,n} \end{pmatrix}$$

Projection

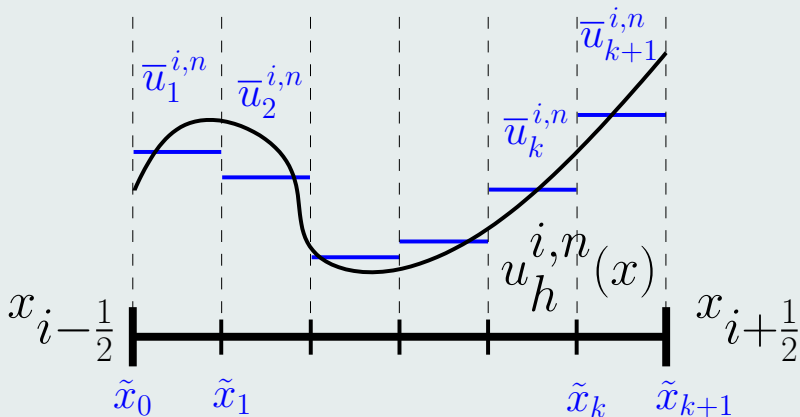


Figure : Polynomial solution and its associated submean values

Set up

- We assume that, for each cell, the $\{\bar{u}_m^{i,n}\}_m$ are admissible
- Compute a candidate solution u_h^{n+1} from u_h^n through unlimited DG
- For each subcell, check if the submean values $\{\bar{u}_m^{i,n+1}\}_m$ are ok

Physical admissibility detection (PAD)

- Check if $\bar{u}_m^{i,n+1}$ lies in an convex physical admissible set (maximum principle for SCL, positivity of the pressure and density for Euler, ...)
- Check if there is any NaN values

Numerical admissibility detection (NAD)

- Discrete maximum principle DMP on submean values:

$$\min_p(\bar{u}_p^{i-1,n}, \bar{u}_p^{i,n}, \bar{u}_p^{i+1,n}) \leq \bar{u}_m^{i,n+1} \leq \max_p(\bar{u}_p^{i-1,n}, \bar{u}_p^{i,n}, \bar{u}_p^{i+1,n})$$

- This criterion needs to be relaxed to preserve smooth extrema

Limited reconstructed flux

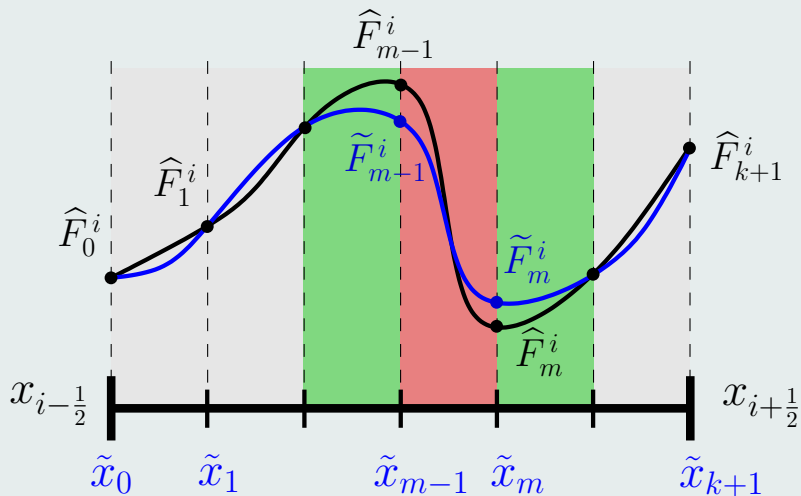


Figure : Correction of the reconstructed flux

Flowchart

- 1 Project $u_h^{i,n+1}$ to get the submean values $\bar{u}_m^{i,n+1}$
- 2 Check $\bar{u}_m^{i,n+1}$ through PAD and NAD
- 3 If $\bar{u}_m^{i,n+1}$ is admissible go further in time, otherwise modify the corresponding reconstructed flux values

$$\tilde{F}_{m-1}^i = \mathcal{F}(\bar{u}_{m-1}^{i,n}, \bar{u}_m^{i,n}) \quad \text{and} \quad \tilde{F}_m^i = \mathcal{F}(\bar{u}_m^{i,n}, \bar{u}_{m+1}^{i,n})$$

- 4 Through the corrected reconstructed flux, recompute the submean values for tagged subcells and their first neighbors
- 5 Return to point 2

Conclusion

- The limitation only affects the DG solution at the subcell scale
- The limited scheme is conservative at the subcell level
- In practice, few submean values need to be recomputed

- 1 Introduction
- 2 DG as a subcell finite volume
- 3 *A posteriori* subcell limitation
- 4 Numerical results**

Initial solution on $x \in [0, 1]$

- $u_0(x) = \sin(2\pi x)$
- Periodic boundary conditions

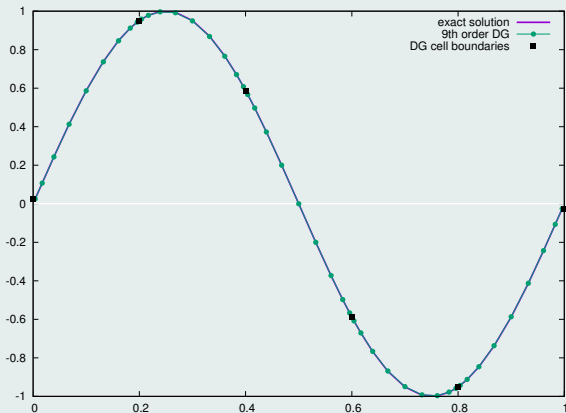


Figure : Linear advection with a 9th DG scheme and 5 cells after 1 period

Convergence rates

	L_1		L_2	
h	$E_{L_1}^h$	$q_{L_1}^h$	$E_{L_2}^h$	$q_{L_2}^h$
$\frac{1}{20}$	8.07E-11	9.00	8.97E-11	9.00
$\frac{1}{40}$	1.58E-13	9.00	1.75E-13	9.00
$\frac{1}{80}$	3.08E-16	-	3.42E-16	-

Table: Convergence rates for the linear advection case for a 9th order DG scheme

Linear advection of a square signal after 1 period

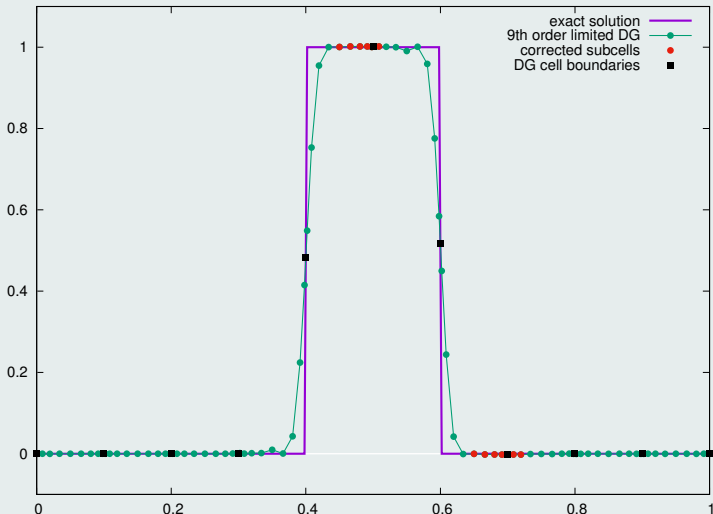


Figure : 9th order limited DG: NAD criterion

Linear advection of a square signal after 1 period

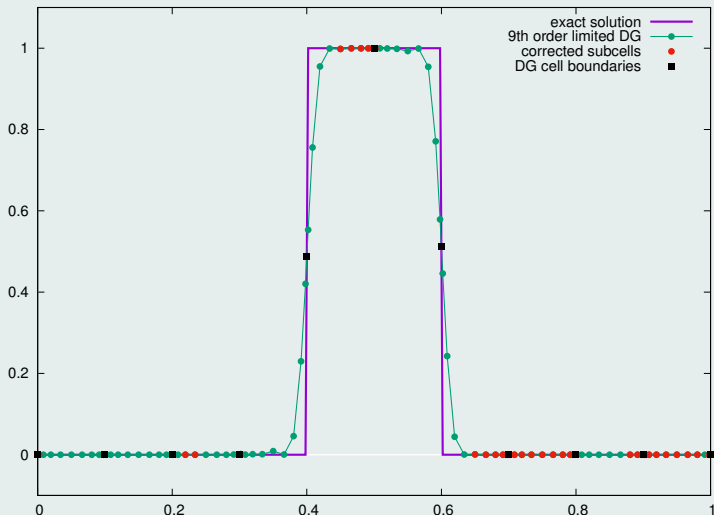


Figure : 9th order limited DG on 10 cells: NAD and PAD criteria

Linear advection of a square signal after 1 period

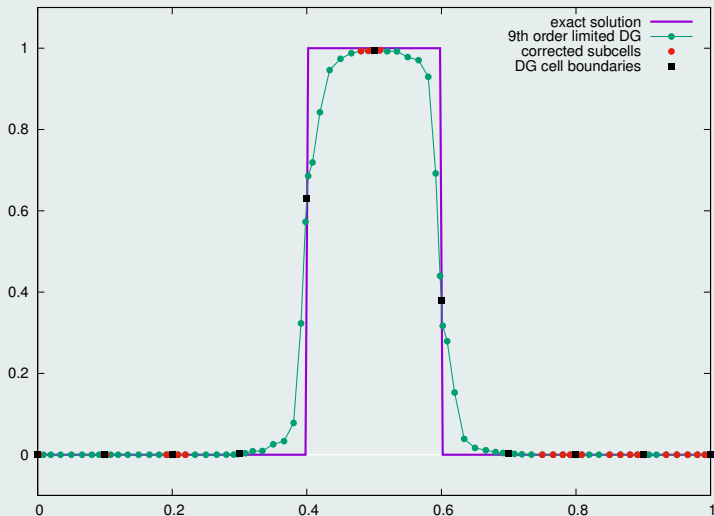


Figure : 9th order limited DG on 10 cells: subcell DMP

Linear advection of a composite signal after 4 periods

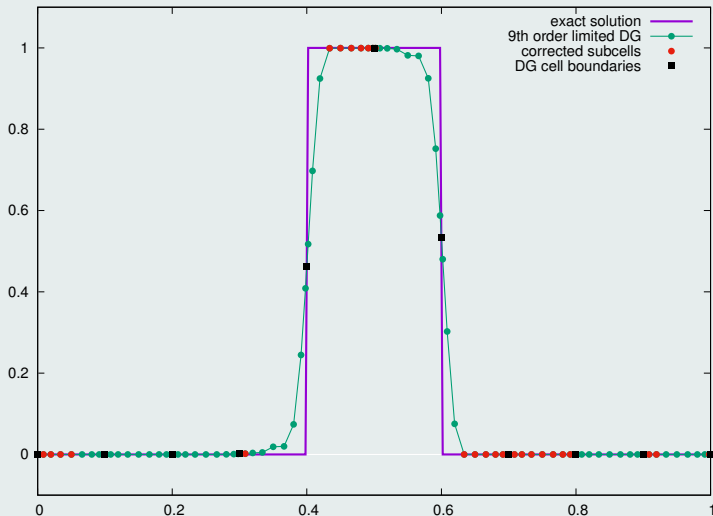


Figure : 9th order limited DG after 4 periods on 30 cells: subcell DMP + 2nd order correction

Linear advection of a square signal after 1 period

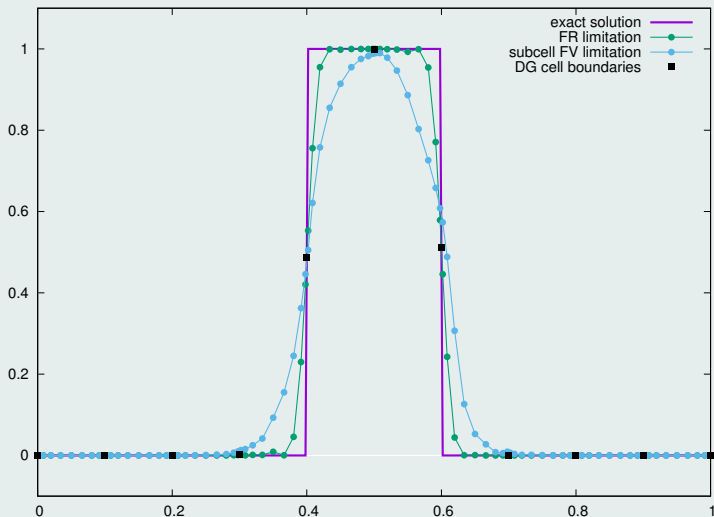


Figure : Comparison between flux reconstruction limitation and subcell finite volume limitation

Linear advection of a square signal after 10 periods

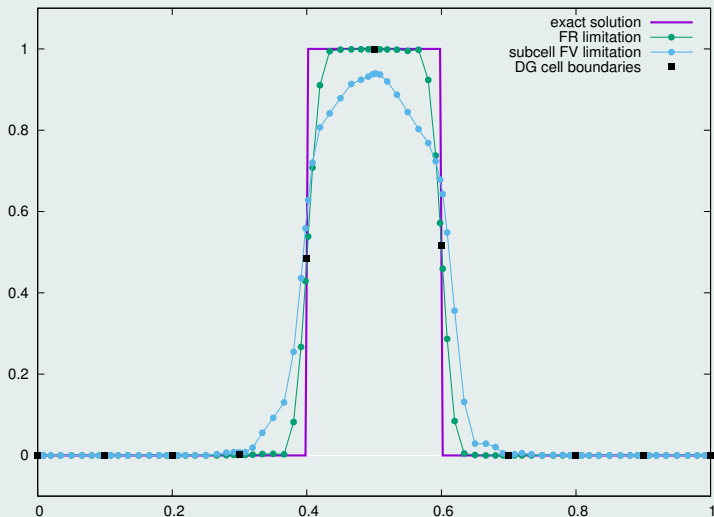


Figure : Comparison between flux reconstruction limitation and subcell finite volume limitation

Linear advection of a square signal after 50 periods

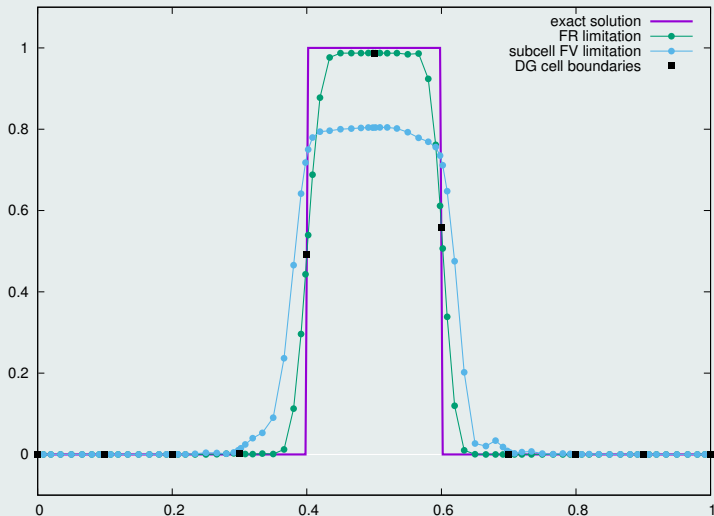


Figure : Comparison between flux reconstruction limitation and subcell finite volume limitation

Linear advection of a composite signal after 4 periods

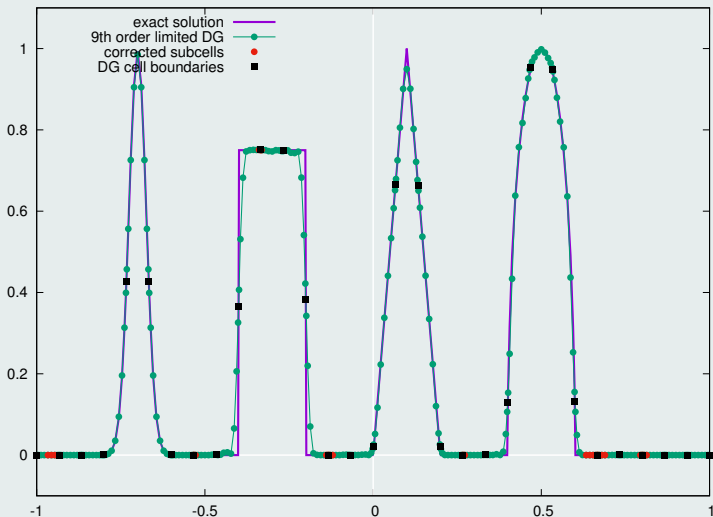


Figure : 9th order limited DG after 4 periods on 30 cells

Linear advection of a composite signal after 4 periods

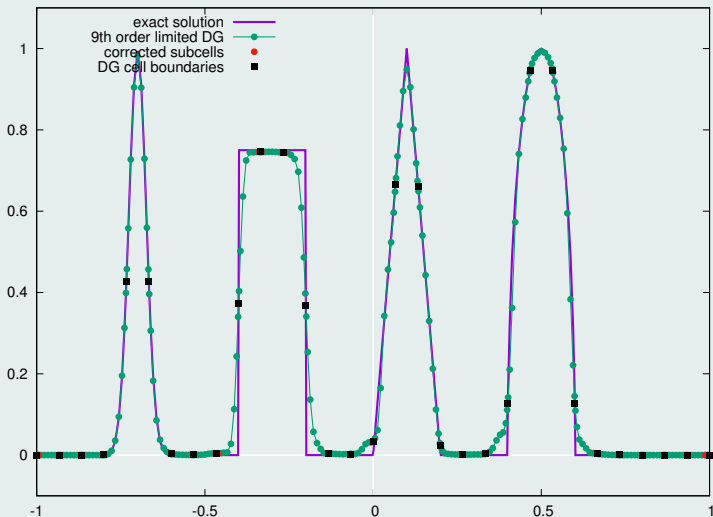


Figure : 9th order limited DG after 4 periods on 30 cells: subcell DMP

Linear advection of a composite signal after 4 periods

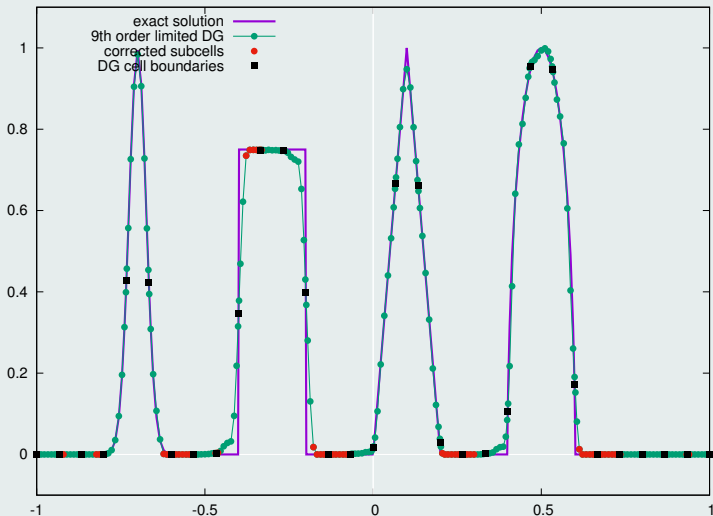


Figure : 9th order limited DG after 4 periods on 30 cells: subcell DMP + 2nd order correction

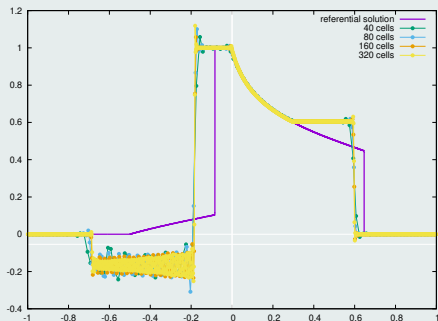
Burgers equation: $u_0(x) = \sin(2\pi x)$

Figure : 9th order limited DG on 10 cells for $t_f = 0.7$

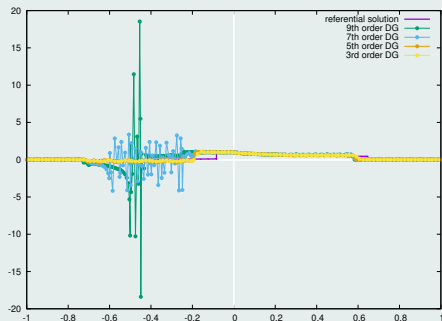
Burgers equation: expansion and shock waves collision

Figure : 9th order limited DG on 15 cells for $t_f = 1.2$

Buckley non-convex flux problem: $F(u) = \frac{4u^2}{4u^2 + (1-u)^2}$



(a) 3rd order DG: non-convergent



(b) DG schemes: aliasing effect

Figure : Unlimited DG schemes

Buckley non-convex flux problem: $F(u) = \frac{4u^2}{4u^2 + (1-u)^2}$

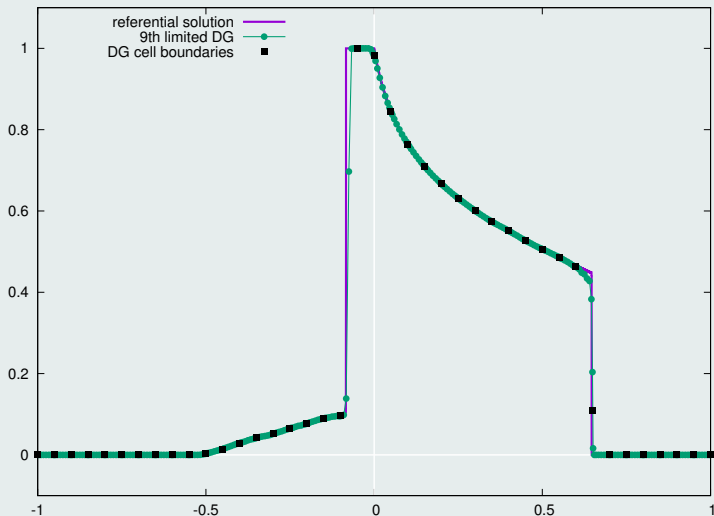
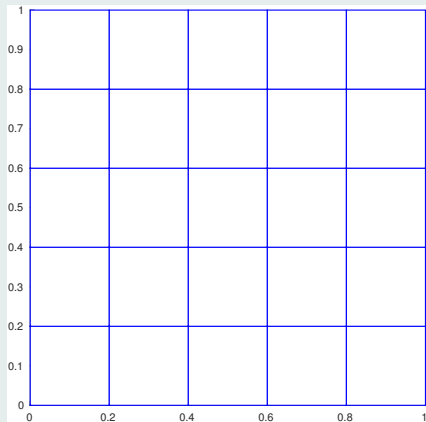
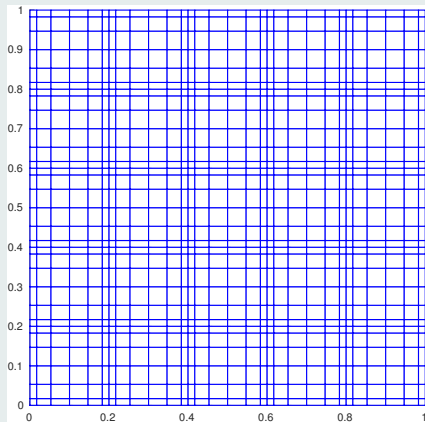


Figure : 9th order limited DG on 40 cells: subcell DMP + 2nd order correction

2D grid and subgrid



(c) Grid

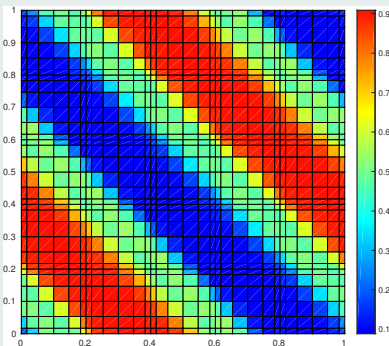


(d) Subgrid

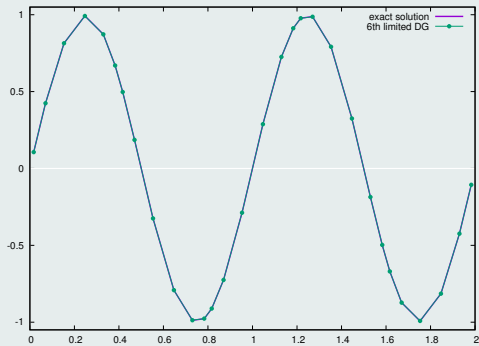
Figure : 5x5 Cartesian grid and corresponding subgrid for a 6th order DG scheme

Initial solution on $(x, y) \in [0, 1]^2$

- $u_0(x, y) = \sin(2\pi(x + y))$
- Periodic boundary conditions



(e) Solution map



(f) Solution profile

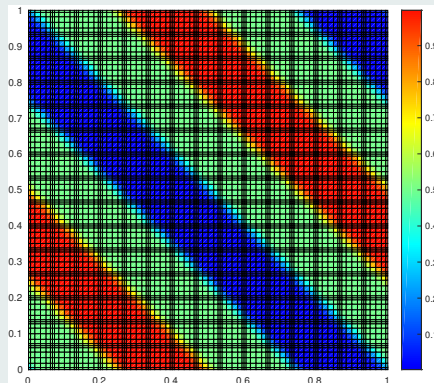
Figure : Linear advection with a 6th DG scheme and 5x5 grid after 1 period

Convergence rates

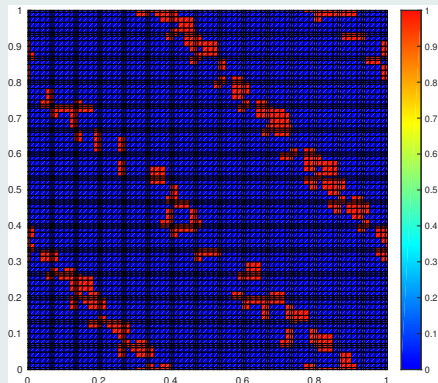
	L_1		L_2	
h	$E_{L_1}^h$	$q_{L_1}^h$	$E_{L_2}^h$	$q_{L_2}^h$
$\frac{1}{5}$	2.10E-6	6.23	2.86E-6	6.24
$\frac{1}{10}$	2.79E-8	6.00	3.77E-8	6.00
$\frac{1}{20}$	3.36E-10	-	5.91E-10	-

Table: Convergence rates for the linear advection case for a 6th order DG scheme

Linear advection of a square signal after 1 period



(g) Solution map



(h) Solution profile

Figure : 6th order limited DG on a 15x15 Cartesian mesh

Linear advection of a square signal after 1 period

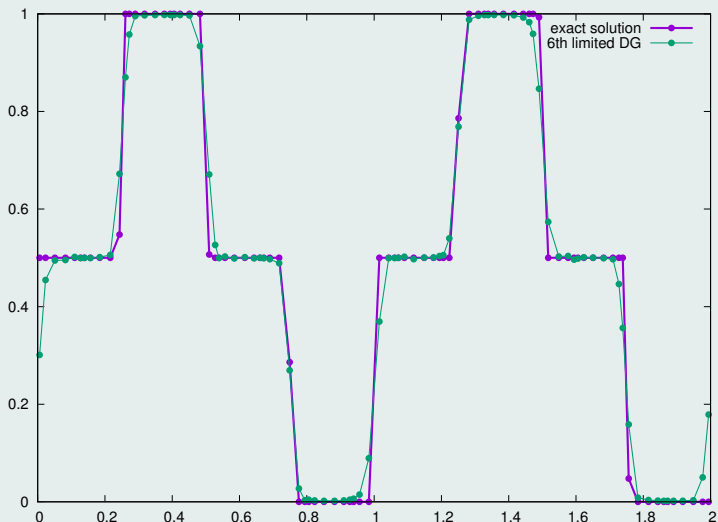
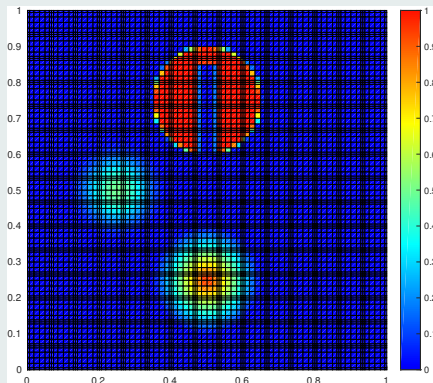
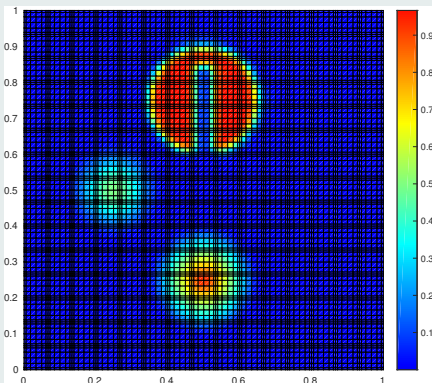


Figure : 6th order limited DG on a 15x15 Cartesian mesh

Rotation of a composite signal after 1 period



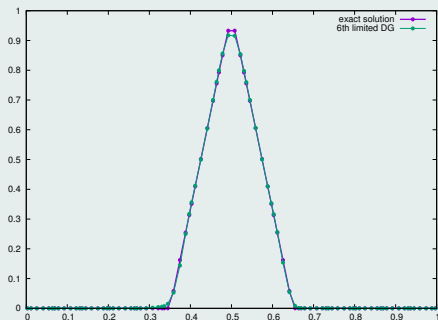
(i) Initial solution



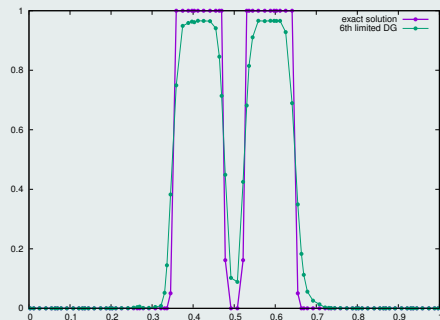
(j) Final solution

Figure : 6th order limited DG on a 15x15 Cartesian mesh

Rotation of a composite signal after 1 period



(k) Solution profile for $y = 0.25$



(l) Solution profile for $y = 0.75$

Figure : 6th order limited DG on a 15x15 Cartesian mesh

Rotation of a composite signal after 1 period: $x = 0.25$

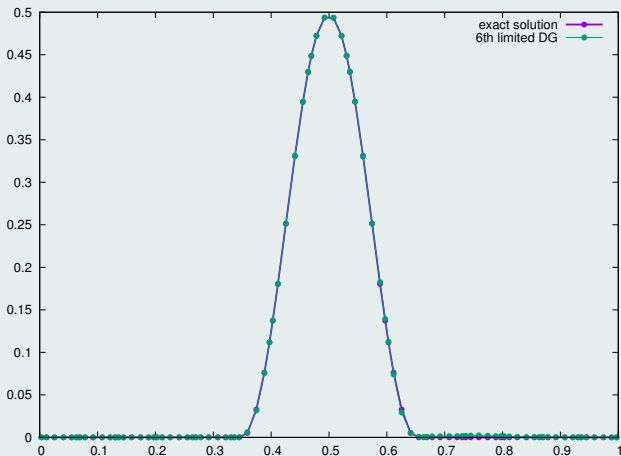
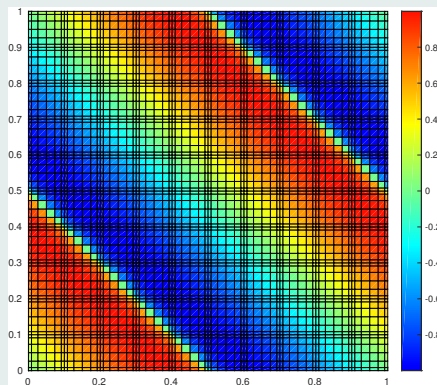
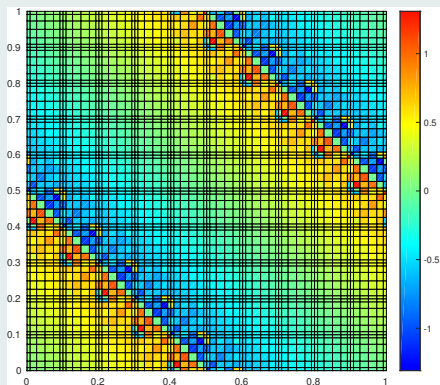


Figure : 6th order limited DG on a 15x15 Cartesian mesh

Burgers equation with $u_0(x, y) = \sin(2\pi(x + y))$



(m) Solution at $t = 0.007$



(n) Solution at $t = 0.25$

Figure : 6th order unlimited DG on a 10×10 Cartesian mesh

Burgers equation with $u_0(x, y) = \sin(2\pi(x + y))$

(o) Solution map

(p) Detected subcells

Figure : 6th order limited DG on a 10x10 Cartesian mesh until $t = 0.5$

Burgers equation with $u_0(x, y) = \sin(2\pi(x + y))$ at $t = 0.5$

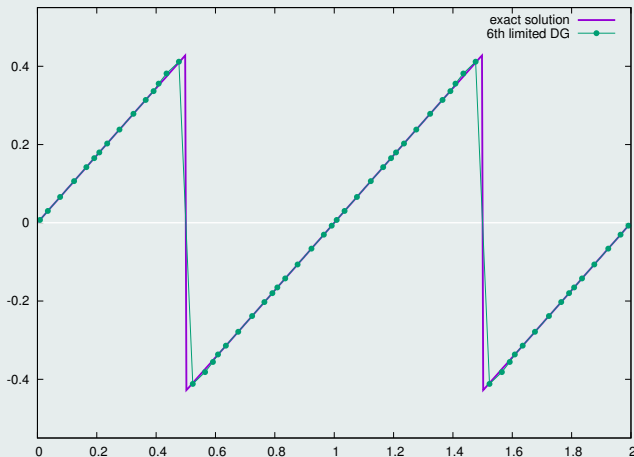
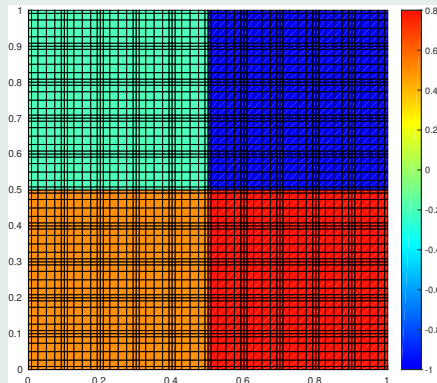
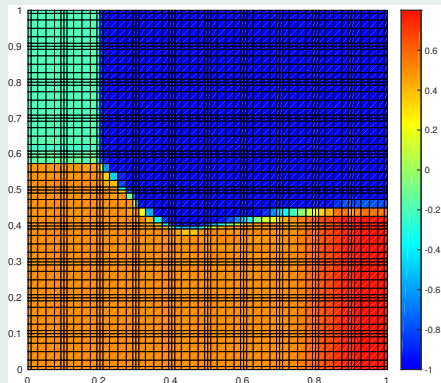


Figure : 6th order limited DG density profile on a 10x10 Cartesian mesh

Burgers equation with composite signal



(q) Initial solution



(r) Solution at $t = 0.5$

Figure : 6th order limited DG on a 10x10 Cartesian mesh

Initial solution on $x \in [0, 1]$ for $\gamma = 3$

- $\rho_0(x) = 1 + 0.9999999 \sin(\pi x)$, $u_0(x) = 0$, $p_0(x) = (\rho_0(x))^\gamma$
- Periodic boundary conditions

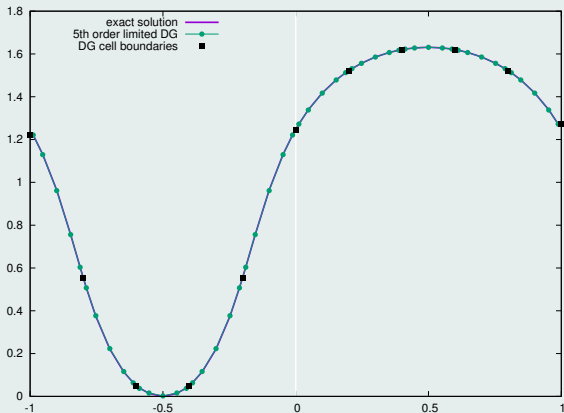


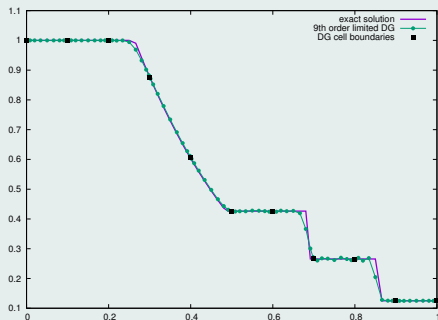
Figure : Smooth flow problem with 5th DG scheme and 10 cells at $t = 0.1$

Convergence rates

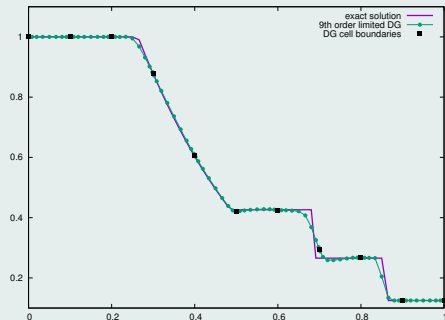
h	L_1		L_2	
	$E_{L_1}^h$	$q_{L_1}^h$	$E_{L_2}^h$	$q_{L_2}^h$
$\frac{1}{20}$	1.48E-5	4.35	2.02E-5	4.18
$\frac{1}{40}$	9.09E-7	4.88	1.38E-6	4.87
$\frac{1}{80}$	3.09E-8	4.95	4.73E-8	4.86
$\frac{1}{160}$	1.00E-9	-	1.63E-9	-

Table: Convergence rates on the pressure for the Euler equation for a 5th order DG

Sod shock tube problem



(s) PAD + NAD



(t) PAD + subDMP with 2nd order correction

Figure : 9th order limited DG on 10 cells

Hell shock tube problem

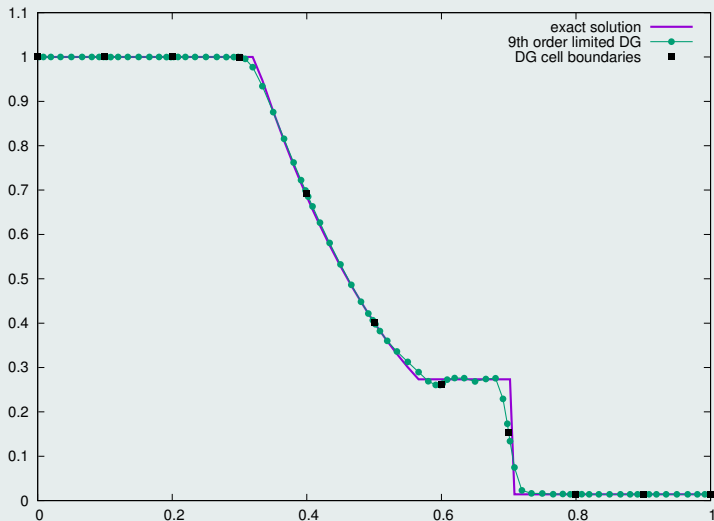


Figure : 9th order limited DG on 10 cells

Shock acoustic-wave interaction problem

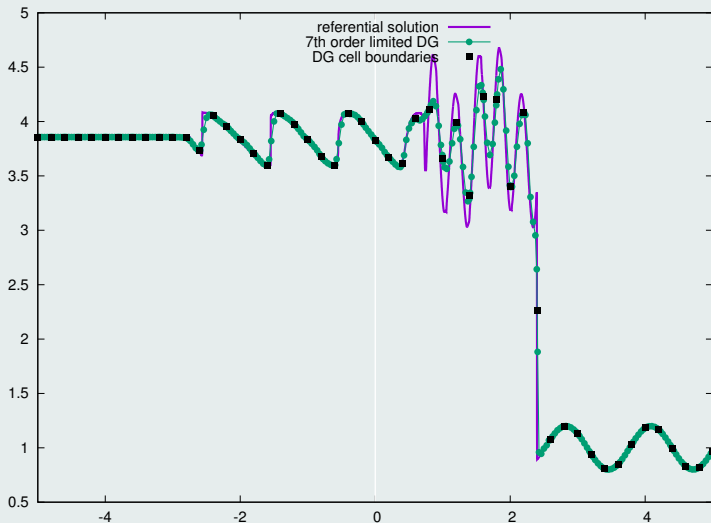
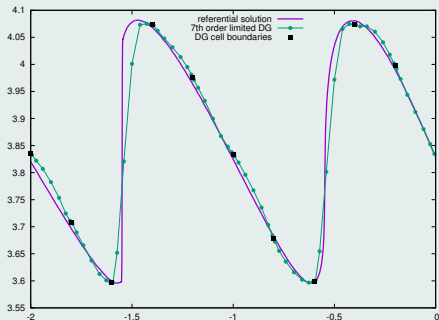
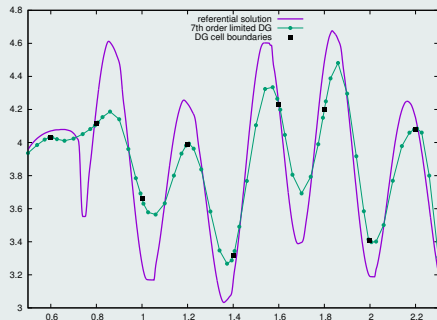


Figure : 7th order limited DG on 50 cells

Shock acoustic-wave interaction problem



(u) Zoom on $[-2, 0]$



(v) Zoom on $[0.5, 2.3]$

Figure : 7th order limited DG on 50 cells

Leblanc shock tube problem

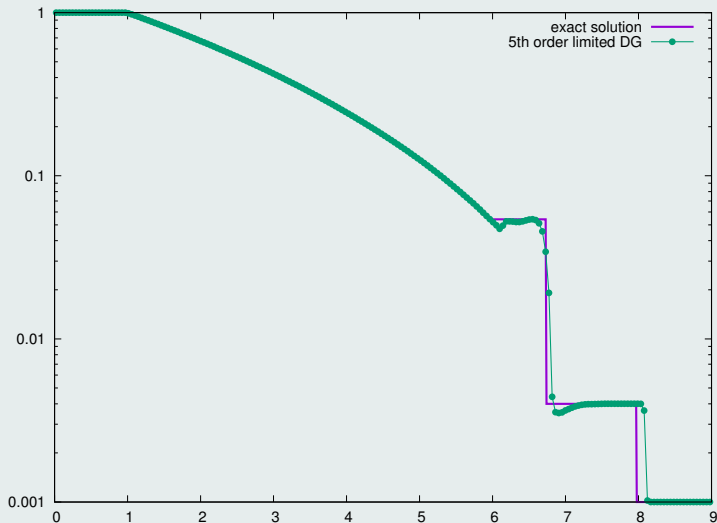


Figure : 5th order limited DG on 200 cells

Article in preparation



F. VILAR, *A Posteriori Correction of High-Order Discontinuous Galerkin Scheme through Subcell Finite Volume Formulation and Flux Reconstruction*. JCP, 2018.

High-order Lagrangian hydrodynamics



F. VILAR, C.-W. SHU AND P.-H. MAIRE, *Positivity-preserving cell-centered Lagrangian schemes for multi-material compressible flows: Form first-order to high-orders. Part II: The 2D case*. JCP, 2016.



F. VILAR, C.-W. SHU AND P.-H. MAIRE, *Positivity-preserving cell-centered Lagrangian schemes for multi-material compressible flows: Form first-order to high-orders. Part I: The 1D case*. JCP, 2016.



F. VILAR, P.-H. MAIRE AND R. ABGRALL, *A discontinuous Galerkin discretization for solving the two-dimensional gas dynamics equations written under total lagrangian formulation on general unstructured grids*. JCP, 2014.

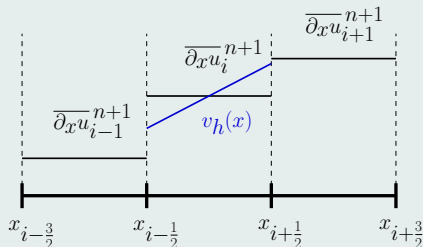
Relaxation of the DMP

- $v_L = \overline{\partial_x u_i}^{n+1} - \frac{\Delta x_i}{2} \overline{\partial_{xx} u_i}^{n+1}$
- $v_{\min \setminus \max} = \min \setminus \max(\overline{\partial_x u_i}^{n+1}, \overline{\partial_x u_{i-1}}^{n+1})$
- If $(v_L > \overline{\partial_x u_i}^{n+1})$ Then $\alpha_L = \min(1, \frac{v_{\max} - \overline{\partial_x u_i}^{n+1}}{v_R - \overline{\partial_x u_i}^{n+1}})$
- If $(v_L < \overline{\partial_x u_i}^{n+1})$ Then $\alpha_L = \min(1, \frac{v_{\min} - \overline{\partial_x u_i}^{n+1}}{v_R - \overline{\partial_x u_i}^{n+1}})$
- $v_R = \overline{\partial_x u_i}^{n+1} + \frac{\Delta x_i}{2} \overline{\partial_{xx} u_i}^{n+1}$
- $v_{\min \setminus \max} = \min \setminus \max(\overline{\partial_x u_i}^{n+1}, \overline{\partial_x u_{i+1}}^{n+1})$
- If $(v_R > \overline{\partial_x u_i}^{n+1})$ Then $\alpha_R = \min(1, \frac{v_{\max} - \overline{\partial_x u_i}^{n+1}}{v_R - \overline{\partial_x u_i}^{n+1}})$
- If $(v_R < \overline{\partial_x u_i}^{n+1})$ Then $\alpha_R = \min(1, \frac{v_{\min} - \overline{\partial_x u_i}^{n+1}}{v_R - \overline{\partial_x u_i}^{n+1}})$

Relaxation of the DMP

- $\alpha = \min(\alpha_L, \alpha_R)$
- If $(\alpha = 1)$ Then DMP is relaxed

Hierarchical limiter



- $v_h(x) = \overline{\partial_x u}_i^{n+1} + (x - x_i) \overline{\partial_{xx} u}_i^{n+1}$

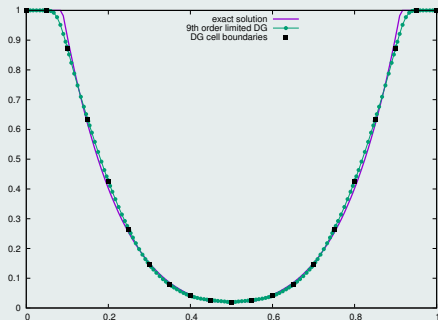


M. YANG and Z.J. WANG, *A parameter-free generalized moment limiter for high-order methods on unstructured grids*. AAMM., 2009.

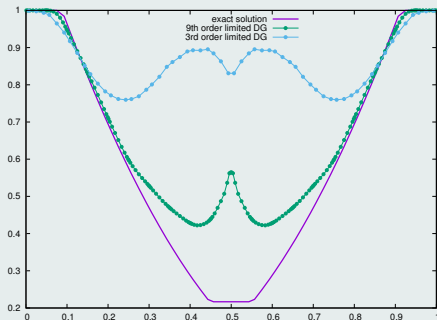


D. KUZMIN, *A vertex-based hierarchical slope limiter for p-adaptive discontinuous Galerkin methods*. J. of Comp. and Appl. Math., 2010.

Double rarefaction problem



(w) Density



(x) Internal energy

Figure : 9th order limited DG on 20 cells